Noise reduction through periodic serial side branches containing two defects

Mohamed El Malki[1*], *Nelson* Pereira[2], Senen Lanceros-Mendez[2,3,4]

[1]Laboratory of Materials, Waves, Energy, and Environment, Department of Physics, Faculty of Sciences, Mohammed First University, Oujda 60000, Morocco
[2]Centro/Departamento de Fisica, Escola de Ciências, Universidade do Minho, Braga, 4710-057, Portugal
[3]Basque Center for Materials, Applications and Nanostructures, UPV/EHU Science Park, Leioa, 48940, Spain
[4]IKERBASQUE, Basque Foundation for Science, Bilbao, 48009, Spain

Abstract. Noise pollution is a challenging issue requiring the development of acoustic systems that can reduce noise. Besides the environmental impacts of noise pollution, it can cause serious health problems. This work originally discusses noise reduction using a new configuration of side branches grafted in series with different terminations. The combination of two serial resonators shows acoustic coupling effects. This effect is used to increase localized modes of two serial defective resonators located in the middle of the structure. The transmission of acoustic waves can be controlled by the dimensions of the introduced defects as well as their boundary conditions. We also show that defects can totally filter the transmission of the pass-bands. The proposed structure can then play the role of an acoustical filter. ***Keywords*.** Noise pollution, Side branches, Acoustic coupling effects, Localized modes, Acoustical filter.

1 Introduction

Noise pollution is not only an environmental issue but also can have important impacts on health. According to the WHO, traffic-related noise accounts for over 1 million healthy years of life lost annually leading to illness, disability, or early death in the western European countries [1]. An important study shows that sleep disturbance can occur if there are a level of 50 dB(A) indoors or more in 50 noise events per night [2]. The use of periodic structures is one of the ways to reduce noise. The increase of periodic structure's interest in photonic crystals extends the idea to other wave propagation phenomena. As a result, several electronic and optical devices have been studied and encourage the application of the same ideas to acoustic phenomena to develop new noise filtering devices taking advantage of band gaps.

Acoustic filters reduce the noise by many ways such as the use of different impedances which cause reflections of the acoustic waves and attenuation. Most of

* Corresponding author: m.elmalki@ump.ac.ma

these filters are based on resonators. In a piping system, acoustic filters are discontinuities
in the structure inducing significant reflections. These discontinuities can be in form of an open pipe termination or a closed branch [3-5]. The acoustic response of such filters has been widely discussed [6-19]. At low frequencies, the electrical diagram equivalent to a side-branch can be made up of two inductors in series [20-21], these last represent the effect of anti-symmetrical modes on the side-branch. The electrical diagram can also consist of an impedance, representing the effect of the plane mode, in series with an inductance representing the effect of the higher modes. The equivalent electric circuit of a symmetrical lateral branch is obtained by Dubos using the modal decomposition [22]. However, the circular geometry presented difficulties. Several tests like the influence of the distance between the side branches, the resonator's length, the pressure and the angle between the branches, have been carried out to study the effect of the flow and geometrical parameters on the acoustic response of two side-branches [23]. The resonance of the two resonators is found to be more important when compared with a single branch under similar test conditions. The difference is due to the acoustic coupling effect between the two side branches which drastically reduces the acoustic radiation into the main duct.

Side branches have an important applications in aeronautical and marine systems [24-28]. Series arrangements of a closed termination resonators were used to reduce synchronous turbo noise. It has been shown that the presented one-dimensional model (1D) gives acceptable results, where the two resonant frequencies and their maximum values were analysed by Allam [29]. However, there is even offset at high frequency and in presence of flow due to the complexity of the chamber of the resonators which brings a 3D effects.

The objective of this work is the study of the propagation of acoustic waves through a new association of serial resonators based on side branches with different terminations. This structure is called the combination of closed and open resonators (CCOR). The parallel configuration of the CCOR system, in which the two different side branches are connected one in front of the other is discussed [30]. The presence of defects inside the periodic parallel resonators shows the influence of acoustic coupling modes of defects.

In this study, we extend our research on CCOR to examine another configuration in which the two side branches are connected in series. The acoustic performance of this new configuration is originally presented using the interface response theory [31]. The boundary conditions of the serial side branches are different. In addition, we focus on the existence of the localized modes inside the forbidden bands due to the presence of two serial defects inside the structure as the effect of one defective resonator is already studied [32]. The coupling effect given by defect modes is examined. The localized mode's transmission are controlled by the modification of the sections of the defects. The analytical and numerical results are validated by those obtained by the transfer matrix method.

2 Theoretical model

2.1 General case of a periodic structure of series of different side branches

In this section, we theoretically study the attenuation of sound through the CCOR system in serial configuration. Side branches are often used in industrial and building extraction and supply networks, in order to prevent the noise generated by acoustic sources from reaching the duct outlet. The behaviour of the acoustic wave in the latter depends essentially on the dimensional property of the guide as well as the boundary conditions of its

termination. The ducts behave like acoustic waveguides. When the wavelength is significantly large, the wave motion can be considered as a plane wave, which offers great simplifications. The plane wave plays an important role in the understanding of the involved physical phenomena.

The proposed configuration is given by two serial resonators (or side branches) along a rectangular waveguide (Figure. 1). The boundary conditions are respectively the vanishing acoustic velocity $u = 0$ at the termination of the closed resonator (medium 2), and the vanishing acoustic pressure ($p \approx 0$) at the termination of the open-side resonator (medium 3). The impedance of the output medium (the radiation impedance) in the open resonator is not taking into account. The two serial resonators are grafted periodically along the main guide.

The Green's function $g^{-1}(M, M)$ of the elementary cell formed by two serial resonators is written in the interfaces space $M = \{0, d_1\}$ as:

$$g^{-1}(M,M) = \begin{pmatrix} -2\frac{F_1C_1}{S_1} - \frac{F_2S_2}{C_2} & -\frac{F_1}{S_1} \\ -\frac{F_1}{S_1} & -2\frac{F_1C_1}{S_1} - \frac{F_3C_3}{S_3} \end{pmatrix} \quad (1)$$

where $F_i = -j\omega/z_i (j = \sqrt{-1}, i = 1-3)$, $C_i = \cosh(k_i d_i)$ $S_i = \sinh(k_i d_i)$, , $k = \omega/c_0\omega$ is the angular frequency of the incident acoustic wave, c_0 the speed of sound speed, and z_i being the characteristic acoustic impedance of the medium *i*.

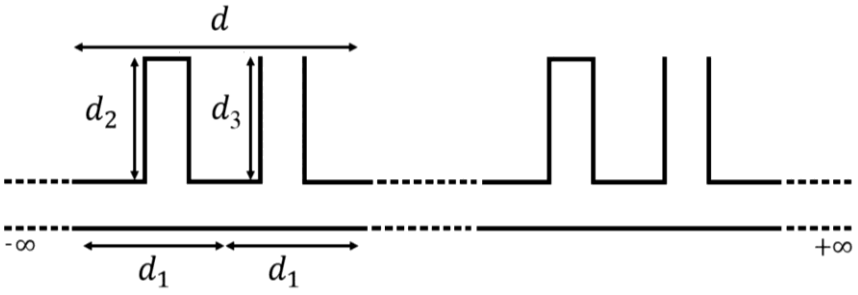

Fig. 1. Diagram of the geometry of the 1D periodic structure formed by serial resonators periodically grafted and separated from each other by a length d_1, $d = 2d_1$ being the period.

$g_\infty^{-1}(M, M)$ of the infinite periodic structure is given by the following matrix:

$$g_\infty^{-1}(M,M) = \begin{pmatrix} \ddots & \vdots & \vdots & \\ \frac{F_1}{S_1} & g^{-1}(1,1) & \frac{F_1}{S_1} & \\ & \frac{F_1}{S_1} & g^{-1}(2,2) & \frac{F_1}{S_1} \\ & \ddots & \ddots & \ddots \end{pmatrix} \quad (2)$$

with $g^{-1}(1,1) = -2F_1C_1/S_1 - 2F_2S_2/C_2$ and $g^{-1}(2,2) = -2F_1C_1/S_1 - F_3C_3/S_3$.

The dispersion relation of the infinite serial resonators is given by:

$$\det\left[\mathrm{g}^{-1}(\mathbf{K}, MM)\right] = \begin{vmatrix} -2\frac{F_1}{S_1} - \frac{F_2 S_2}{C_2} & \frac{F_1}{S_1} + \frac{F_1}{S_1}\mathrm{e}^{(-\mathrm{jKd})} \\ \frac{F_1}{S_1} + \frac{F_1}{S_1}\mathrm{e}^{(\mathrm{jKd})} & -2\frac{F_1 C_1}{S_1} - \frac{F_3 C_3}{S_3} \end{vmatrix} = 0 \quad (3)$$

Where K is the Block wave number. Assuming that the acoustic structure is constructed with the same material, the dispersion relation is given by:

$$\cos(\mathbf{K}d) = \cos(k_1 d) - \frac{1}{2} z_1 [y_2 \tan(k_2 d_2) - y_3 \cot(k_3 d_3)] \sin(k_1 d) + \frac{1}{2} z_1^2 y_2 y_3 \sin^2\left(\frac{k_1 d}{2}\right) \tan(k_2 d_2) \cot(k_3 d_3) \quad (4)$$

This equation is similar to the equation obtained in [32] using the transfer matrix. Using this later, the transmission loss of the serial side branches is given by

$$\mathrm{TL} = 10 \log|1 + (z_1 y_R/2)|^2 \quad (5)$$

where

$$y_R = \frac{B_2}{A_2} \quad (6a)$$

$$A_2 = AA_0^2 + y_{op} BA_0^2 + A_0 BC_0 + y_c AA_0 B_0 + y_c y_{op} A_0 BB_0 + y_c BB_0 C_0 + A_0 B_0 C + y_{op} A_0 B_0 D + B_0 C_0 D \quad (6b)$$

$$B_2 = AA_0 C_0 + y_{op} A_0 BC_0 + BC_0^2 + y_c AA_0 B_0 + y_c AA_0 D_0 + y_c y_{op} A_0 BD_0 + y_c BC_0 D_0 + A_0 CD_0 + y_{op} A_0 DD_0 + C_0 D_0 A_0 DD_0 + C_0 DD_0 \quad (6c)$$

$$A = \cos(k_1 d_1) \quad (7a)$$
$$B = \mathrm{j} z_1 \sin(k_1 d_1) \quad (7b)$$
$$C = \mathrm{j} y_1 \sin(k_1 d_1) \quad (7c)$$
$$D = \cos(k_1 d_1) \quad (7d)$$
$$A_0 = \cos(k_1 d_1/2) \quad (7e)$$
$$B_0 = \mathrm{j} z_1 \sin(k_1 d_1/2) \quad (7f)$$
$$C_0 = \mathrm{j} y_1 \sin(k_1 d_1/2) \quad (7j)$$
$$D_0 = \cos(k_1 d_1) \quad (7k)$$
$$y_{op} = -\mathrm{j} y_3 \cot(k d_3) \quad (7l)$$
$$y_c = \mathrm{j} y_2 \tan(k_1 d_2) \quad (7m)$$

y_{op} and y_c are the acoustic impedances of the open side resonator and the closed resonator, respectively.

3 Numerical results

3.1 Transmission loss coefficient of serial side branches

Figure 2 represents the variation of the transmission loss coefficient through serial closed and open-side branches connected along a rectangular waveguide. One can clearly observe the two resonance frequencies corresponding to these resonators. Since the open resonator is a high-pass filter, the first peak corresponds to the latter. The behaviour of high-pass filter of the open resonator dominates. To identify the origin of the second resonance, we varied the length of the closed resonator (d_2) for a fixed value of d_3. The second resonance (TL = 60) located at frequency 1317Hz moves towards lower frequencies as d_2 increases. While the first peak remains the same. This confirms that

this resonance corresponds to that of the closed resonator.

To take advantage of the configuration of the serial resonators, an arrangement of closed resonators have been experimentally examined by Allam [29]. The numerical results show that the transmission loss of the overall system exhibits a combined behaviour that superimposes the two peaks provided by the gated resonators in a non-overlapping frequency range. This result shows that cascading different resonators in the resonator design can achieve more attenuation performance, provided the resonators are properly designed and optimized to be effective in different frequency bands.

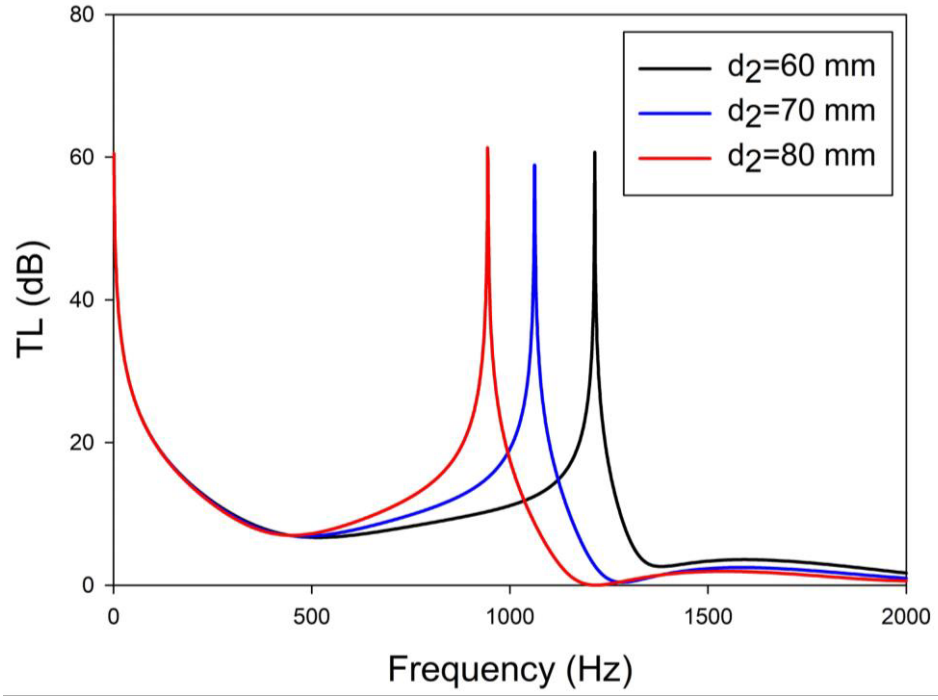

Fig. 2. The transmission loss coefficient of serial open and closed resonators branched in series for different values of d_2. Case where $d_2 = d_3 = 60$mm and $s_2 = s_3 = \pi 25^2 mm^2$.

3.2 Transmission of the periodic structure of serial side branches containing two dimensional defects

Here, we study the appearance of localized modes inside the structure which contains the compound defects of the closed and open resonator in a series configuration (Figure 3). The resonators and the main tube are filled with air. We note that the geometries of all the grafted side branches, including the defects, consist of cylindrical sections, while the main tube has a square cross-section ($50 \times 50 mm^2$). The transmission coefficient of the defective structure is calculated using the transfer matrix [32]. The simulation results are based on experimental data obtained from literature.

As a unit cell is composed of two serial side-branches, the defect can be one of the two resonators corresponding to the central cell located. Therefore, the defect of the resonator can have a closed, an open end or both.

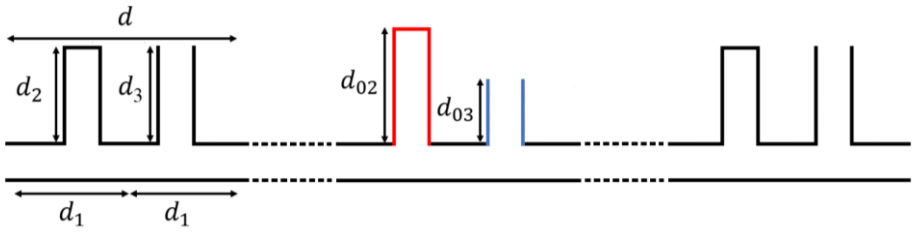

Fig. 3. Diagram of the geometry of a periodic structure formed by periodically grafted serial resonators in the presence of defects in the form of a closed and open resonator. The two resonators are grafted into the same central cell along an acoustic waveguide.

3.3 Effect of the presence of one defective resonator inside the periodic side branches

We should consider the effect of the presence of one defective resonator that is already discussed [32] which can make the interpretation of the coupling effect of the two defects modes more clear. The defective resonator can be in form of closed or open-side branch in the middle of the structure. Figure 4 shows the effect of the presence of the defective open resonator. This can be achieved by changing the dimension (cross-section) of the open resonator, located in cell n = 5. The other resonator, located in the same cell, is similar to the common closed side branches. The transmission coefficient of the perfect structure is presented in Figure 4(c).

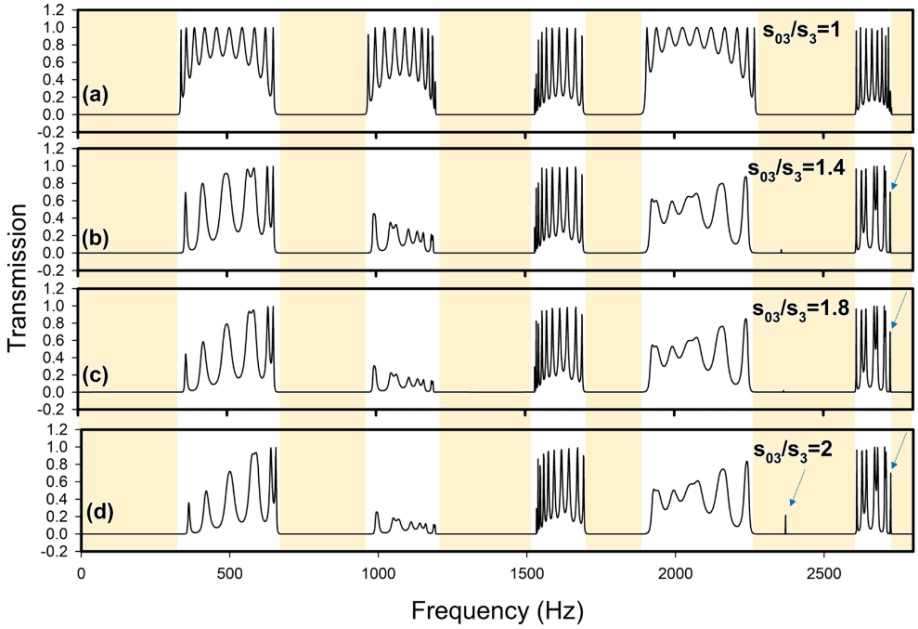

Fig. 4. Variation of the transmission coefficient as a function of the section ratio s_{03}/s_3. The defect take the form of an open-side branch located in the central cell n = 5 for 10 identical unit cells, $d_{03}/d_3 = 0.5$, $d_{02}/d_2 = 1$, $s_2 = s_{02} = \pi 25^2 mm^2$ [32].

A localized mode appears in the fifth band gap. As the cross-section of the defective open resonator increases, the peak shifts to higher frequencies. Its reaches the middle of the fifth band gap while keeping low transmission below 0.50. Inside the sixth band gap, notably the limit of the fifth pass-band, a localized mode of amplitude T = 0.69 appears at a fixed position. This peak is located on frequency 2724Hz and is not affected by the variation of s_{03}. This type of localized mode is also observed in the parallel configuration resonators [30].

The fourth pass band is affected by the insertion of the defective open resonator. For $s_{03}/s_3 > 1$, the transmission inside the first pass-band is also decreased (Figure 4(d)-(f)). With a defective open resonator, most of the second pass-band transmission is attenuated, especially in the case where $s_{03}/s_3>1.4$ (Figure 4(j)-(f)). These remarks bring us back to the conclusion that this structure can play the role of an acoustic filter rather than a selective filter since the localized mode inside the structure has a very weak transmission. However, the high-pass character of the defective open resonator shifts the localized mode towards high frequencies, this is not the case for the parallel configuration of the CCOR system which contains a defective open resonator [30].

Figure 5 shows the effect of the presence of a defective closed resonator inside the periodic side branches. The defect of the closed resonator of different section replaced the closed resonator located in the middle of 10 identical cells.

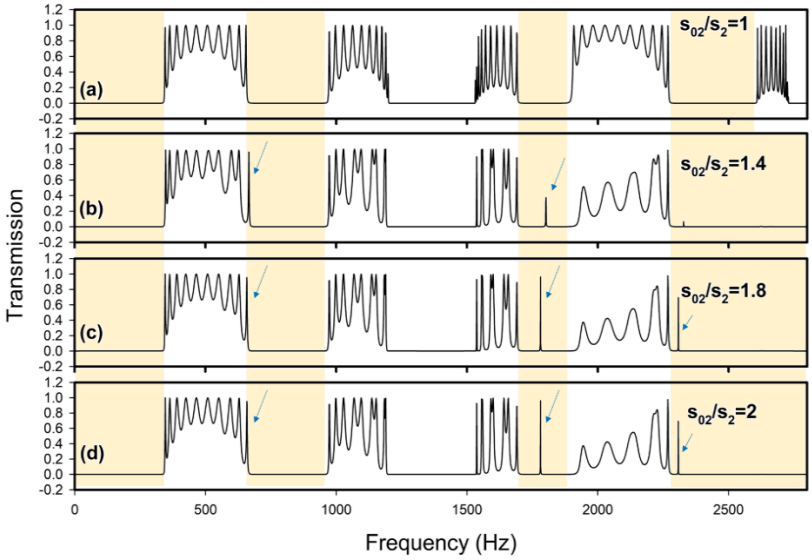

Fig. 5. Variation of transmission coefficient as a function of section ratio s_{02}/s_2. The defect is in form of a closed resonator located in the middle of 10 identical unit cells, $d_{02}/d_2 = 0.5$, $d_{03}/d_3 = 1$, $s_3 = s_{03} = \pi 25^2 mm^2$ [32].

As the defective cell contains two different resonators, the second one (the open resonator) is similar to the common open resonators. A localized mode of strong transmission appears in the second band gap. By increasing the section of the defect (s_{02}), this localized mode moves towards low frequencies. It goes from 685Hz for $s_{02}/s_2 = 0.4$ to 658Hz for $s_{02}/s_2 = 2$. The same remark is observed on the fourth forbidden band where the defect mode passes from the limit of the fourth

forbidden band (Figure 5(a)) to the limit of the third pass-band (Figure 5(f)). This peak moves through the entire fourth band gap. The transmission decreases when the section closes to that of common open resonators. This peak becomes more important as the section becomes larger. The direction of defect mode shift in this case towards low frequencies. This is the opposite of what is observed in the case of defective open resonator (Figure 4). This behaviour is due to the fact that the closed resonator works as a low pass filter. Hence, the defective closed resonator acts as a selective filter that can shift the mode towards low frequencies.

A localized mode located at the frequency 1537Hz appears inside the third band gap with high transmission (T = 0.90). This peak is not affected by the variation of the defective section. Also, a localized mode on the frequency 2308Hz appears inside the fifth forbidden band for $s_{02}/s_2 > 1.4$.

A significant influence of the defective closed resonator appears inside the fifth pass-band in which the entire pass-band is depressed giving rise to a large band gap. This new forbidden band is caused by the Eigen-frequency of the defect which falls on the pass-band. The pass-bands are also affected by the presence of the defect, in particular the fourth pass band (Figure 5(f)).

3.4 Effect of the presence of two serial defects inside the CCOR

After presenting the case of a one defect inside the CCOR system, we present the study of the effect of inserting two defects with two different terminations inside the periodic side branches which is the main objective of this investigation. The two serial resonators corresponding to the central cell are dimensional defects (closed and open resonator in series) with two different cross-sections. The identification of the localized modes of the two defects requires, for instant, the length of one of the two defects to be fixed.

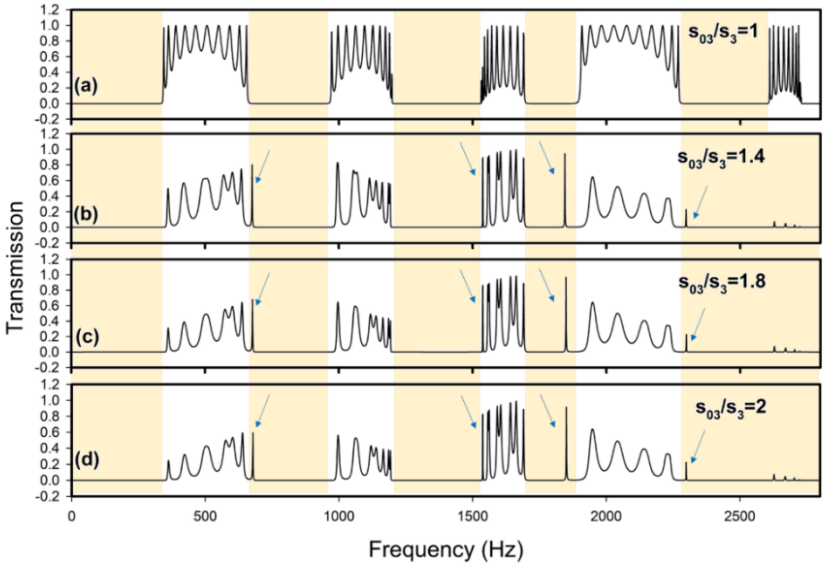

Fig. 6. Variation of the transmission coefficient as a function of the section ratio s_{03}/s_3. The two defects are in the form of a closed resonator and an open resonator with a fixed length ($d_{03}/d_3 = 0.5$). The two serial defects are located in the middle of 10 identical unit cells for $d_{02}/d_2 = 0.5$ and $s2 = \pi 25^2 mm^2$.

Let's consider the case where $d_{02}/d_2 = 0.5$. Fig
ure 6 shows the transmission spectrum of the periodic structure of the closed and open-side branches in series in the presence of a defect of the closed resonator and that of the open resonator. The study is made by varying the cross-section of the open resonator which is given by the section ratio s_{03}/s_3. Since the presence of a single defective open resonator shows a localized modes with weak transmission. The objective is therefore to evaluate the same defect in the presence of a second defect with a different boundary condition (closed resonator). It is a way to examine the effect of interactions between defect modes. At the second band gap, a localized mode of high transmission and fixed frequency appears (676Hz). The transmission of this mode decreases when the section of the defective open-side branch becomes larger than that of common open resonators ($s_{03}/s_3 > 1$). Since the presence of a defective open resonator (Figure 5) shows no localized mode inside the second gap, and considering the fact that the position of this mode is located on the frequency 676Hz, we can conclude that this mode comes from the fixed defective closed resonator. Another remark confirms our conclusion is the fact that the position of the localized mode frequency in the case of a single defective closed resonator (Figure 5(a)) is 685Hz for $s_{02}/s_2 = 0.4$, this frequency is very close to the position of the localized mode observed for two defects (Figure 6(a)). This confirms a coupling effect between the two defect modes. Moreover, the decrease of the localized mode transmission for $s_{03}/s_3 > 1$ is due to the variation of s_{03}. The latter is also decreases the transmission of the first pass-band. This behaviour is similar to that of a single defective open resonator (Figure 4(d)-(f)). On the other hand, the two defects contribute to the attenuation of transmission waves inside the fourth pass-band. The defect of the open-side branch has no effect on the reduction of the transmission of the third pass-band. This is mainly caused by the defect of the closed side-branch.

In the third forbidden band, a localized mode appears, its transmission 0.90 at a fixed frequency equal to 1537Hz. It is exactly that of the defect of the closed resonator (Figure 5). Moreover, this peak does not appear in the absence of the defective open resonator (Figure 6(c)) which confirm our remark. The defect mode due to the section variation of the defective closed resonator also appears in the fourth forbidden band, its transmission increases as the section s02 increases. This transmission remains fixed for $s_{02}/s_2 > 1$.

The defect mode corresponds to the defective open resonator appears in the middle of the fifth forbidden band (Figure 6(b)). Its frequency is close to that obtained by a single defective open resonator (Figure 4) with very low transmission (T = 0.35). This case is the only one where the localized mode of this defect is observed. On the other hand, the localized mode of the defective closed resonator appears to the left of that of the defective open resonator (Figure 6(b)). Its transmission remains fixed at the position 2296Hz which is very close to that observed in Figure 5. Half of the transmission of this peak is attenuated due to the variation of the defective section of the open resonator. If we compare this transmission with that illustrated in Figure 5(e), we can remark that the transmission of the defective open resonator goes from 0.69 to 0.22 (Figure 6(e)).

The defect of the closed resonator has destroyed the entire transmission at the level of the fifth pass-band, this is a behaviour already described in Figure 5 as a result of the coupling effect of defect modes. The series configuration of the CCOR system gives very useful results. In fact, this configuration shows two characters of selection of the defect modes obtained by different filters in particular that of low and high frequencies. The selection of modes in two different

directions (towards low and high frequencies) is presented here in an original way. This way of selecting modes is only possible thanks to the CCOR system.

4 Conclusion

We theoretically presented an original study of a 1D periodic CCOR composed of two different side branches grafted along a rectangular acoustic duct. The infinite periodic structure has wide acoustic band gaps that can be used in noise reduction, these band gaps come from both closed and open-side branches. The band structure of the perfect CCOR system shows that the combination of the filters has the character of a high-pass filter, this behaviour is mainly imposed by the open-side branches.

The behaviour of the localized modes is analysed by varying the cross-section of the defective closed resonator in the case where the length of the defective open resonator is fixed. We show that both defects contribute to give rise to the localized modes. These results are very important and show the coupling effect of defects. In particular, when they are caused by two different filters. Moreover, the transmission of pass-bands is also affected by the presence of defects. In fact, by introducing a defective open-side resonator, we are able to attenuate the transmission inside pass-bands.

In the case of a single defective open resonator, the direction of defect mode displacement is towards high frequencies, which is the opposite of that obtained by a single defective closed resonator. The low/high filtering of frequencies appears clearly in the CCOR of series configuration. The presence of the defects therefore makes it possible to exploit the forbidden frequency regions. We showed that defect modes can change their movement direction depending on the boundary condition of the defective resonator. Thus, the new configurations proposed in this study can play the role of a selective filter of low or high frequencies. The transmission of acoustic waves can be controlled by the dimensions of the introduced defects as well as their boundary conditions.

References

1. WHO. Regional Office for Europe, (2011)
2. S.A. Stansfeld, M.P. Matheson, Br. Med. Bull. 68, 243–257 (2003), 10.1093/bmb/ldg033
3. D. Tonon, B. Landry, S. Belfroid, J. Willems, G. Hofmans, A. Hirschberg, JSV **329**, 1007–1024 (2010), https://doi.org/10.1016/j.jsv.2009.10.020
4. D. Tonon, J. Willems, A. Hirschberg, JSV **330**, 5894–5912 (2011), https://doi.org/10.1016/j.jsv.2011.07.024
5. D. Tonon, *Aeroacoustics of shear layers in internal flows: closed branches and wall perforations* (2011), DOI: DOI: 10.6100/IR716254
6. U. Ingard, H. Ising, JASA **42**, 6–17 (1967), https://doi.org/10.1121/1.2143575
7. D. Ronneberger, JASA **24**, 133–150 (1972)
8. A. Cummings, W. Eversman, JSV **91**, 503–518 (1983)
9. P. Davies, Practical flow duct acoustics, JSV **124,** 91–115 (1988)
10. P. Durrieu, G. Hofmans, G. Ajello, R. Boot, Y. Aurégan, A. Hirschberg, M. Peters, JASA **110**, 1859–1872 (2001)
11. S. Boij, B. Nilsson, JSV **260,** 477–498 (2003), https://doi.org/10.1016/S0022-460X(02)00950-1
12. S. Boij, B. Nilsson, JSV **289**, 577–594 (2006), https://doi.org/10.1016/j.jsv.2005.02.017

13. S. Boij, JASA **126,** 995–1004 (2009)
14. G. Kooijman, A. Hirschberg, Y. Aurégan, JSV **329,** 607–626 (2010), DOI: https://doi.org/10.1016/j.jsv.2009.09.021
15. G. Kooijman, P. Testud, Y. Aurégan, A. Hirschberg, JSV **310,** 902–922 (2008), https://doi.org/10.1016/j.jsv.2007.08.008
16. A. Khettabi, D. Bria, M. Elmalki, JMES **8,** 816–824 (2017)
17. A. Khettabi, M. Elmalki, *Analytical study by transfer matrix and green's method of a periodic lattice formed by dual Helmholtz resonators (DHR)*, in Proceedings of International Conference on Electrical and Information Technologies (ICEIT), IEEE, 1–3, (2017), 10.1109/EITech.2017.8255268
18. M. Elmalki, A. Khettabi, *Study of various periodic acoustic lattices by two methods: Transfer matrix and green's method*, in Proceedings of International Conference on Electrical and Information Technologies (ICEIT), IEEE, 1–3, (2017), DOI: 10.1109/EITech.2017.8255269
19. M. El Malki, A. Khettabi, *Application of the interface response theory to a periodical expansion chambers*, in AIP Conference Proceedings, **2074**, 020025, AIP Publishing LLC, (2019), https://doi.org/10.1063/1.5090642
20. D.H. Keefe, Theory of the single woodwind tone hole, JASA **72**, 676–687 (1982)
21. V. Dubos, J.-P. Dalmont, J. Kergomard, J. Phys. IV **4**, C5–279 (1994)
22. V. Dubos, *Etude de l'effet d'une cheminee laterale sur un guide d'onde acoustique. Etude theorique de l'interaction de deux cheminees* [*Study of the effect of a lateral chimney on an acoustic waveguide. Theoretical study of the interaction of two chimneys*], (Doctoral dissertation, Le Mans, 1996).
23. S. Ziada, E. Bühlmann, J. Fluids Struct. **6**, 583–601 (1992)
24. F.C. Demetz, T.M. Farabee, *Laminar and turbulent shear flow induced cavity resonances*, in Proceedings of Aeroacoustics Conference, 4th, Atlanta, Ga, American Institute of Aeronautics and Astronautics, 14, (1977)
25. S.A. Elder, JASA **64**, 877–890 (1978).
26. S.A. Elder, T.M. Farabee, F.W. Demetz, JASA **72**, 532 (1982).
27. S.P. Parthasarathy, Y.I. Cho, B.L.H, JASA **78**, 1785 (1985).
28. L. East, JSV **3**, 277 – 287 (1966), https://doi.org/10.1016/0022-460X(66)90096-4
29. S. Allam, Sci. and Educ. **1**, 12–23 (2015)
30. M. El Malki, A. Khettabi, *Acoustic wave transmission through periodic parallel resonators*, in Materials Today Proceedings, (2022), https://doi.org/10.1016/j.matpr.2022.09.393
31. L. Dobrzynski, Surf. Sci. Rep. **11**, 139–178 (1990)
32. M. El Malki, A. Khettabi, IJAST **29**, 3330–3340 (2020)